JOURNAL OF MATERIALS SCIENCE 29 (1994) 3678–3690

Ceramic joining III bonding of alumina via Cu/Nb/Cu interlayers

M. L. SHALZ, B. J. DALGLEISH, A. P. TOMSIA, R. M. CANNON, A. M. GLAESER
Center for Advanced Materials, Lawrence Berkeley Laboratory and Department of Materials Science and Mineral Engineering, University of California, Berkeley, California 94720, USA

A method of ceramic–ceramic joining that exploits a multilayer interlayer designed to form a thin, potentially transient layer of liquid phase has been used to join alumina to alumina. Microdesigned multilayer Cu/Nb interlayers were used to achieve bonding at 1150 °C. Flexure strengths of as-bonded samples ranged from 119 to 255 MPa, with an average of $\approx$ 181 MPa. The ability to form 'strong' ceramic/metal interfaces is also indicated by instances of ceramic failure. Microstructural and chemical characteristics of fracture surfaces were evaluated using SEM, EDS and microprobe. The impact of post-bonding anneals of 10 h duration at 1000 °C in gettered argon on room-temperature joint strength was assessed. High strengths (198 to 238 MPa) were obtained. The retention of strength following annealing in low oxygen partial pressure argon differs from the behaviour previously observed in Cu/Pt bonded alumina. Effects of the anneal on interfacial microstructure were determined, and an explanation for this difference in behaviour is proposed.

1. Introduction

Fundamental studies of microstructure–property–processing interrelationships have contributed to the development of advanced structural metals, ceramics, intermetallics and composites of these materials with improved properties and performance. Joining smaller components of such materials to one another will be an essential aspect of fabricating new structures as well. The fabrication of large complex ceramic structures will probably require the joining of smaller components. For other applications, it will be desirable to combine components made of several different materials to form a complex structure with improved or novel properties and function. Structures may be designed in which materials are combined to produce an intentional 'functional' gradient in a material property. Often different regions of a larger structure see vastly differing service conditions, requiring materials with widely varying properties in different regions of the assembly.

When joining dissimilar materials, the thermal expansion mismatch between the materials, their chemical compatibility, and the temperature capabilities of the least refractory member impose processing and joint design constraints. Fundamental studies of, and innovative approaches to joining these materials to themselves and to one another are required to provide the scientific basis for ameliorating such difficulties and processing new structures.

In Parts I and II of this study, the results of using multilayer Cu/Pt/Cu [1] and Cu/Ni/Cu [2] interlayers for partial transient liquid phase (PTLP) joining of alumina to itself were described. The results demonstrated that strong refractory joints with reduced thermal expansion mismatch can be produced at substantially lower temperatures than those required for conventional joining approaches. A more detailed study of the effects of interlayer composition, processing conditions, and post-bonding heat treatments is in progress. The present paper reports the results of an investigation of joining alumina via similarly microdesigned multilayer Cu/Nb/Cu interlayers.

2. Background

Solid-state diffusion bonding and liquid-based reactive metal brazing are thought to be the joining approaches most likely to succeed in producing strong joints for demanding high-stress, high-temperature applications [3–5]. Diffusion bonding allows the fabrication of ceramic/metal/ceramic assemblies using refractory metal interlayers that are unsuitable for brazing. Thus research has demonstrated that strong Pt/Al_2O_3 [6, 7] and Nb/Al_2O_3 [8–12] interfaces can be produced by diffusion bonding, while efforts to braze Al_2O_3 with pure Pt have been unsuccessful [6, 7] and brazing Al_2O_3 with pure Nb is not possible. However, diffusion bonding is not without drawbacks. Although joining temperatures can be as low as 0.5 T_m (where T_m is the absolute melting temperature of the metal) [12], more typically, bonding temperatures of the order of 0.8–0.9 T_m are required to produce optimum bond quality [see e.g. 6–15]. Thus when refractory metals are used, processing temperatures can be high. Achieving complete ceramic–metal contact during bonding can be facilitated by the preparation of smooth and flat bonding surfaces [13, 14],

0022–2461

but this requires additional surface-preparation steps. Finally, a load must be applied during bonding; within limits, bond quality can be improved by increasing the applied load. However, the need to apply a potentially substantial load during bonding limits the joint geometry and may induce distortions in the pieces to be joined.

Liquid-state processing offers greater flexibility in joint configuration, imposes less stringent surface preparation requirements, relieves the need to apply an appreciable load, and lends itself more readily to mass production. However, the success of the method relies on proper wetting of the ceramic by the molten interlayer [3]. Reactive metals such as Ti and Zr can be added to the interlayer to reduce the contact angle [16]; however these metals can also increase the yield stress and thus reduce the ability of the interlayer to accommodate plastically the thermal expansion mismatch stresses that arise during cooling and thermal cycling. Moreover, reaction layers usually develop which, if excessively thick, can lead to strength degradation of joined assemblies, necessitating compromises between wetting, spreading and ultimate mechanical properties.

The problems of developing strong joints by diffusion bonding and brazing are compounded when the intended assembly-use temperature is increased. Use of more refractory metals or brazing alloys increases the processing temperature requirements. Interfacial reactions that are thermodynamically prohibited or kinetically inhibited at lower temperatures, become more probable as the joining temperature is increased [17]. The use of progressively higher-melting-point metals may decrease the mismatch in thermal expansion ($\Delta\alpha$) with the ceramic; however the potential temperature range over which misfit is accumulated (ΔT) may increase as a result of an increase in processing temperature. Finally, the need to process at temperatures that exceed the ultimate use temperature may lead to degradation of the properties of the components to be joined. For example, nickel–base superalloys that are candidate materials for certain components of a 'ceramic' engine will undergo property degradation if exposed to temperatures above 1200 °C for prolonged periods.

Efforts to develop low-temperature joining methods for high-temperature applications have been relatively limited. Iino and Taguchi [18] have proposed an interdiffusing multilayer metal interlayer (IMMI) method as an alternative to conventional solid-state diffusion bonding. The process substantially reduces the temperature requirements for forming a strong bond, while retaining the other advantages of diffusion bonding. Studies demonstrated that through the use of multilayer Ni/Nb/Ni and Nb/Ni/Nb interlayers, strong silicon nitride assemblies could be produced at significantly lower temperatures than when Nb or Ni foils were used alone.

Transient liquid phase (TLP™) bonding has the potential to combine some of the best features of diffusion bonding and brazing. The viability of using TLP bonding for joining nickel–base superalloy components has been demonstrated and the method has been exploited commercially. Refractory bonds with a strength equivalent to that of the base materials that were joined have been achieved [19].

However, the application of TLP bonding to ceramics is limited. Following the pioneering work of Loehman, who used oxynitride glasses for TLP bonding of silicon nitride ceramics [20], subsequent studies examined the role of processing conditions, glass and silicon nitride chemistry, and environmental exposure on the properties and interfacial microstructures of oxynitride glass-bonded silicon nitride [21–24]. Baik & Raj [24] explored the effects of glass chemistry and silicon additions on thermal expansion mismatch and tendencies for frothing of the glass at elevated temperatures. Iseki *et al.* [25, 26] report successful joining of reaction-bonded SiC using Ge interlayers. In this case, the excess Si (≈ 12 wt %) in the SiC acts as a more refractory sink for Ge, evolving into a Si-rich Si-Ge solid solution.

In conventional TLP bonding the entire interlayer is molten, and a favourable interaction between the molten interlayer and the adjoining ceramic (or bulk metal) is required to transform the interlayer into a more refractory material at the bonding temperature. The earliest effort to develop a multilayer metal interlayer for joining in which only a portion of the interlayer becomes molten may be that by Bernstein & Bartholomew [27]. Their work employed a metal preform with a laminated structure, a low-melting-point material (In, Sn) clad on a higher-melting-point core (Au, Ag, Cu, Ni), to produce bonds that were capable of withstanding temperatures higher than those at which the bond was made, typically 300 °C. They focussed on demonstrating the applicability of this method, which they referred to as solid–liquid interdiffusion (SLID) bonding, to integrated-circuit fabrication. Brief reference is made to the formation of an Ag–In bond to a nickel-plated Mo–Ti metallized alumina. More recent efforts by Iino [28] and by Glaeser and co-workers [1, 2, 29–30] have also focussed on the development of multilayer metal interlayers for ceramic–ceramic joining in which only a portion of the interlayer becomes molten. Iino has used the term partial transient liquid phase (PTLP) brazing to describe this variation on TLP bonding.

PTLP brazing retains the advantages of TLP bonding, and provides new flexibility in defining the properties of the interlayer and reducing the required bonding temperature. Through suitable use of equilibrium phase diagrams, multilayer metal interlayers with 'self-contained' low-melting-point transient liquid phases can be designed. This approach permits brazing which utilizes refractory-metal-based interlayers. The use of refractory metals will often reduce the interlayer–ceramic thermal expansion mismatch, and the use of a lower-melting-point cladding to some extent decouples the choice of the interlayer expansion coefficient from the processing temperatures required to achieve the joint. In principle, interlayers can be tailored to meet the needs of a broad range of material combinations spanning high-temperature structural and lower temperature electronic device applications.

A more detailed discussion of PTLP bonding has been provided in [1], and thus the concept will be explained only briefly here. In contrast to bonding methods in which a chemically homogeneous interlayer is used, both the IMMI and PTLP bonding methods rely on an inhomogeneous interlayer. Specifically, a thin film of a low-melting-point metal or alloy is deposited onto a much thicker foil of a more refractory metal or alloy, or directly onto the ceramic. Bonding is conducted at a temperature that lies above the minimum liquidus temperature in the system. In previous joining work using Cu/Pt/Cu interlayers, a processing temperature of 1150 °C was used to bond alumina. Cu and Pt exhibit complete mutual solubility at elevated temperature, and thus at temperatures above the melting point of Cu one expects disappearance of the Cu-rich liquid due to diffusion of Cu into Pt. Pt was selected because of its excellent thermal expansion match with alumina, and excellent oxidation resistance. Cu and Ni also exhibit complete mutual solubility in the solid state at high temperatures, and Cu/Ni/Cu interlayers have also been used to join alumina successfully [2].

In the present work, Cu was retained as the basis for the transient liquid phase because of (i) its relatively lower melting point (1085 °C), (ii) its ease of deposition, (iii) considerable prior research on Cu–Al_2O_3 diffusion bonding [31–35] and brazing [36–40], (iv) prior fracture studies of Cu/Al_2O_3 interfaces [15, 32, 33, 35–40], and (v) the success of prior PTLP bonding research with Cu [1, 2].

Nb was selected as the refractory metal host. Nb has a high melting point ($\approx$ 2470 °C) and closely matches the thermal expansion of alumina. Thus Nb is an interlayer of choice when thermal expansion mismatch must be small. Numerous studies of Nb/Al_2O_3 diffusion bonding and Nb/Al_2O_3 interfaces are available in the literature [e.g. 8–12, 41–53], and the fracture of bonded assemblies has been studied extensively [8–12, 41]. Measurements of strength against temperature have been conducted, and it has been suggested that Nb-bonded Al_2O_3 assemblies could be useful to temperatures as high as 1500 °C in non-oxidizing atmospheres [8].

Prior work on PTLP bonding with Nb used a Sn-rich alloy as the basis for the partial transient liquid phase (M. Locatelli & A. M. Glaeser, unpublished data). The Nb–Sn phase diagram has three intermetallic phases, $NbSn_3$, Nb_6Sn_5, and Nb_3Sn [54]. The combination Cu–Nb appeared to be a more attractive alternative because there are no brittle intermediate phases in the system, and at temperatures above the melting point of Cu, the composition of the equilibrium liquid contains a few atomic percent of Nb [55]. It was anticipated that Nb might play the role of a reactive metal, and have a beneficial effect on the wetting behaviour of the transient liquid.

Some uncertainty existed regarding phase equilibrium in the Cu–Nb system. Phase equilibrium studies conducted during the 1950s and reported in the compilation of Elliot [55] indicated a maximum solubility of Cu in Nb of 15 at % at the monotectic temperature of 1550 °C, a solubility of 9 at % Cu in Nb at a peritectic temperature of 1100 °C, and solubility of $\approx$ 4 at % Cu in Nb at lower temperature. A system with these characteristics would be an excellent candidate for PTLP bonding. More recent phase diagram studies suggest that the Cu–Nb system is typical of systems in which compositional impurities have a strong modifying effect on the equilibrium phases both in the liquid and solid state. When low oxygen content niobium was employed in phase equilibrium studies, the phase relationships of a eutectic phase diagram were observed, and a much lower maximum solubility of Cu in Nb ($\approx$ 1.2 at % at 1080 °C) was indicated [54]. If the more recent results proved germane to our study, the relatively lower solubility of Cu in Nb, coupled with the expected low diffusion rate of Cu in Nb would make this system less attractive for PTLP bonding than Cu–Pt. Nonetheless, although our results showed extremely limited incorporation of Cu in Nb, robust joints were produced.

3. Experimental procedures

3.1. Materials

A 99.5% pure, $\gtrsim$98% dense alumina (Coors, Golden, Colorado, USA) with a bimodal grain size distribution (with the larger mode at $\approx$ 25 μm) was machined into 19.5 × 19.5 × 22.5 mm^3 blocks. Blocks were machine-polished to a 1-μm (grit size) finish, and subsequently cleaned in isopropyl alcohol, and blown dry. Cleaned blocks were placed in an alumina crucible (99.5% purity), covered, and then annealed in air at 1000 °C for 14 h with the bonding surface exposed to the crucible atmosphere to remove organic contaminants from the surface; this also leads to discernible thermal etching of the grain boundaries.

Foil interlayers 20 × 23 mm were cut from a larger 127-μm-thick 99.99% pure Nb sheet, cleaned ultrasonically in 2-propanol, then rinsed in ethanol followed by a rinse in nanopure water (resistivity 18.3 MΩ cm). Excess water was wicked from the foil edges while the foil was blown dry with the hot air gun. The cleaned and dried foil was stored in a wafer dish (used in microelectronics processing) until needed.

Experiments examining the wetting behaviour of pure Cu and Cu-rich Cu–Nb alloys on alumina used a high purity (99.9999% pure), oxygen-free high conductivity copper source as the base material. The copper was cleaned in a 10% nitric acid solution, given multiple rinses in distilled water, and then dried. Small pieces of high-purity Nb of known total weight were pressed into the copper rods to produce an overall composition of Cu–2 wt % Nb. This corresponds roughly to the liquidus composition at 1150 °C indicated in recent phase diagrams.

3.2. Sessile drop experiments

Wetting experiments were conducted at 1150 °C in a Ta element furnace. Rods of pure Cu and of the Cu–Nb mixture were placed onto adjacent, identical, polished and cleaned alumina substrates. For the Cu–Nb rods, the Nb-embedded end was placed in contact with the alumina. The two samples were

heated simultaneously at a rate of 10 °C min^{-1} to 1150 °C while a vacuum of 5 to 7×10^{-6} torr was maintained. Alloying occurred *in situ*. The total time at temperature was 2 h. During the anneal, the contact angles on both sides of each sessile drop were measured periodically using a telegoniometer with a precision of $\pm 2°$.

3.3. Copper coating

Thin layers of copper were deposited onto both alumina blocks by evaporating a commercial copper wire (Consolidated Companies Wire and Associated, Chicago, Illinois, USA). Cleaned copper wire segments were premelted in tungsten wire baskets under a vacuum of $2–9 \times 10^{-6}$ torr. The polished and cleaned alumina blocks were placed into the evaporator, and copper coated. The chamber pressure was reduced to $\approx 3 \times 10^{-6}$ torr, and fluctuated between 7 and 10×10^{-6} torr during deposition.

A copper layer ≈ 3 μm thick was deposited onto each substrate. The copper thickness was measured using two methods. One method is based on a determination of the weight gain per unit area of an adjacent glass cover slip. The other relies on using a profilometer to measure the step height produced where a portion of glass slide was masked with a cover slip. Both measurements indicate an average Cu thickness of ≈ 3 μm, with some variation in thickness indicated by profilometry. This average thickness implies an average interlayer composition of $\gtrsim 93$ at % Nb.

3.4. PTLP bonding

Bonding was performed in a vacuum hot press. The block/foil/block stack was assembled immediately after the completion of coating and loaded into a graphite hot-pressing die. After an adequate vacuum was achieved, the temperature was ramped to 1150 °C at 4 °C min^{-1}, maintained at 1150 °C for 6 h, and then ramped down to room temperature at 2 °C min^{-1}. During this cycle, the vacuum in the press was in the range of $0.8–2 \times 10^{-5}$ torr. A pressure of ≈ 5.1 MPa was maintained on the assembly during the entire cycle. This represents the minimum positive load that can be applied to the sample using the hot press available. It is likely that a significantly lower load would suffice.

3.5. Beam preparation

Five plates were cut from the bonded block assembly using a diamond wafering saw. The plates were numbered so that any systematic trends in strength, or in the appearance of fracture surfaces, could be related to the original position in the block assembly. Subsequently, one surface of each plate was polished prior to sectioning the plates into beams for flexure testing. All plates (1 to 5) were hand polished on plate glass with 30-μm diamond, and then polished for 100 h with 15-μm diamond in an oil slurry on a vibratory polisher. To determine whether an improved surface finish would improve strength, one plate (4) was given an additional 2-h polish with 6-μm diamond, and two plates (2 and 3) were polished for 23 h with 6-μm diamond.

Beams of approximately square cross section ($\approx 3.4 \times 3.4$ mm) were cut from the polished plates with the metal interlayer at the beam centre. The tensile edges of flexure beams were bevelled to remove machining flaws that could initiate failure. Beams cut from the same plate are referred to as a set of beams.

3.6. Post-bonding heat treatments

Beams from plate 5 were annealed for 10 h at 1000 °C in > 99.998% purity argon (oxygen-gettered with a mixture of titanium and zirconium chips) to determine whether further chemical homogenization of the interlayer and environmental exposure affected the flexure strength. In Cu/Pt/Cu samples [1], an identical heat treatment caused a severe loss of strength, and microstructural evidence suggests that interfacial dewetting of the metal layer occurred.

3.7. Flexure testing

Beams were tested at room temperature using four-point bending. The inner span was 8 mm. Testing was done with a displacement rate of 0.05 mm min^{-1}. Strengths were calculated from the load at failure using standard relationships derived for monolithic elastic materials, i.e. no correction for stress concentrations arising from modulus misfit [56, 57] was attempted. Prior work had determined that under identical testing conditions, the four-point bend strengths of (unbonded) alumina beams prepared from the same source material are ≈ 280 MPa (B. J. Dalgleish, unpublished data).

3.8. Microstructural and microchemical characterization

After mechanical testing, beam fracture surfaces were mounted adjacent to one another so that equivalent fractographic locations were in mirror symmetry positions. The general microstructure at matching locations, the pore structure, and the fracture path could thus be readily identified. Fracture surfaces were first inspected using optical microscopy, and then examined using scanning electron microscopy (SEM). Although some pullout of the ceramic occurred during failure, fracture proceeded primarily along one ceramic-metal interface. The surface containing the metal interlayer is termed the metal side of the fracture surface, the opposing one the ceramic side. The metal side of selected fractured beams was etched in a 1 part-by-volume (1.40 specific gravity) nitric acid, 3 parts by volume 40% hydrofluoric acid mixture for ≈ 8 s and then rinsed in distilled water. This revealed Nb grain boundaries.

Residual plates trimmed from the edges of the bonded blocks were polished and examined using energy dispersive spectroscopy (EDS) to evaluate the extent of diffusion of copper into niobium during the

complete bonding cycle. Line scans were conducted perpendicular to the interface. The electron beam diameter is typically of the order of 1 μm, and a typical detection limit is ≈ 1 at %, and thus we anticipated this method might provide information on the extent of homogenization achieved during the bonding cycle. Although no data were found for diffusion of Cu in Nb, qualitatively one would expect a reduced penetration relative to that observed for Cu in Pt. In the event that the equilibrium solubility of Cu in Nb is as low as indicated in recent phase diagrams, it was also anticipated that removal of copper from the interface region might be incomplete for the processing conditions used.

4. Results

4.1. Fracture strength

Beams from plates 1–4 were tested to determine the as-processed failure strength, and its dependence on tensile surface preparation. Nominally, the quality of the surface finish increased in the order 1 → 4 → (2, 3). Thus, if polishing induced flaws were determining the strength, one might anticipate that strengths would increase in the same order. However, prior work has indicated that the flaws causing failure in the alumina employed are of the order 10–15 μm in size, and thus, polishing beyond the 15 μm level would have limited benefit.

The strength data for as-processed bend specimens are in Table 1. The samples prepared from plate 1 had consistently high strengths; the mean was 249 MPa with a standard deviation of ± 5 MPa. With increasing polishing, the mean strength for any set of similarly processed samples decreased to values between 150–165 MPa, and the standard deviation increased relative to that for plate 1 samples. Thus, the additional polishing, cleaning, and handling appears to impact strength deleteriously.

A mapping of the spatial distribution of bend strengths within the block is shown in Fig. 1. The strength distributions for as-processed and argon-annealed Cu/Nb/Cu bonds are also shown in the strength–probability plots of Fig. 2, which includes the strength distribution of similar size beams of unbonded alumina and an upper limit on the strength of argon-annealed Cu/Pt/Cu bonds. In the present work, the argon-annealed samples, which were also given the minimal surface preparation, have strengths nearly as high as those of samples cut from plate 1. This supports the interpretation that excessive polishing and the associated ultrasonic cleaning, or some combination of the two can degrade joint strength.

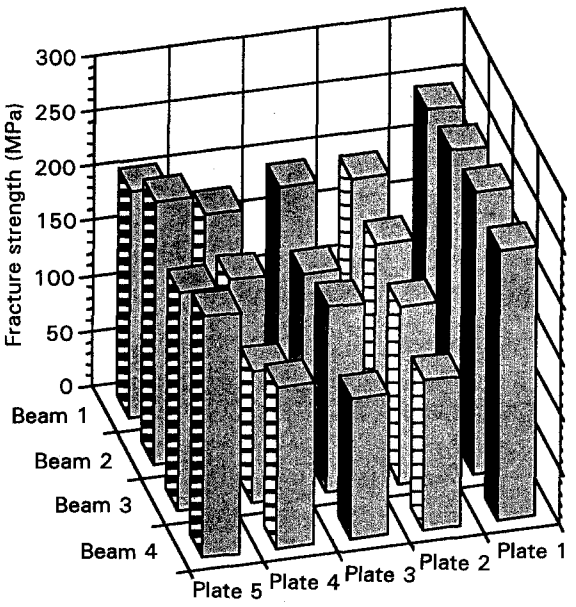

Figure 1 Spatial distribution of bond strengths.

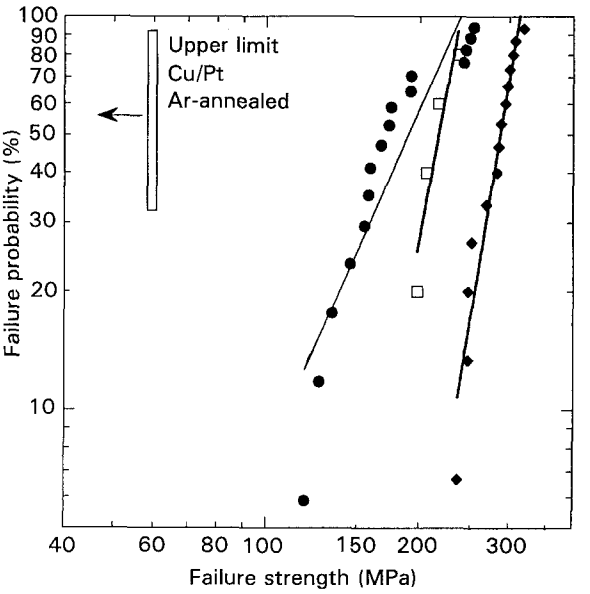

Figure 2 Failure probability against failure strength for Cu/Nb/Cu bonded assemblies and data for argon-annealed Cu/Pt/Cu interlayers [1] for comparison. Reference data for unbonded beams prepared from the same alumina are included. ●, As-processed; □, Ar-annealed; ◆, unbonded Al_2O_3.

Coincidentally, plates 1 and 5 are edge plates, and the highest strength samples within plates 2, 3, and 4 all come from one edge. (This can be seen easily in Fig. 1). Crowning of samples during polishing is widely observed. As a result, ceramic–metal contact is not

TABLE I Flexure strengths (MPa)

Surface preparation	Plate	Beam 1	Beam 2	Beam 3	Beam 4	Mean	Standard deviation
100 h vibratory polish with 15-μm diamond	1	**246**	**251**	**255**	**244**	249	5
As plate 1 + 23 h vibratory polish with 6-μm diamond	2	**192**	174	160	135	165	24
As plate 2	3	**192**	156	168	127	161	27
As plate 1 + 2 h vibratory polish with 6-μm diamond	4	**176**	159	119	146	150	24
As plate 1 + 10 h anneal at 1000 °C in Ar	5	**206**	**238**	**198**	**218**	215	17

The bold numbers indicate the high strength beams which tend to lie along three of the sample edges.

uniform, and in solid-state bonding, pore removal is often most difficult near the edges. In the present case, when the thin layer of liquid is formed, liquid redistribution may occur, expedited by the imposed bonding pressure. Chemical analysis and fractographic studies were used in an effort to assess whether variations in liquid thickness occurred, and could be correlated with strength differences.

4.2. Fractography and chemical analysis

The microstructure and microchemistry of fracture surfaces of selected as-processed beams (including that exhibiting the lowest (119 MPa), an intermediate (192 MPa) and the highest (255 MPa) failure strength), and one beam subjected to post-bonding annealing were examined using optical microscopy, SEM and EDS.

Fracture in all samples examined was predominantly interfacial, and thus the microstructures on the metal and ceramic sides of the fracture path could be compared. Several features distinguish the low strength and high strength samples. In both samples, the crack occasionally enters the ceramic and is then drawn back to the interface. As shown in Fig. 3, there is an increased degree of ceramic pullout in the higher strength samples. Fig. 3a and b show the metal side of the fracture surface of a high- and low-strength sample, respectively. The lower edge in each micrograph corresponds to the tensile edge of the bend beams. Although the failure origin in the stronger sample was not identified, the tensile edge shows that fracture occurred largely through the ceramic. Fig. 4 illustrates that in the regions of ceramic failure, both intergranular and transgranular fracture occur. The fracture strength of the higher strength samples approaches that of the ceramic. The differences in the crack path suggest that there is a spatial variation in the strength of the ceramic–metal interfacial bonding, with higher interfacial strengths promoting more extensive temporary excursions of the crack into the ceramic component, and possibly crack initiation in the ceramic.

Optical microscopy of fracture surfaces suggests that some redistribution of copper occurred; in some beams, primarily those from the block edge, discrete regions accounting for $< 10\%$ of the fracture surface were copper-coloured. There was a greater tendency for ceramic failure in those regions where (unreacted) copper was more common, and copper was generally evident around the pullout region perimeter. In areas where the adhered alumina layer was sufficiently thin, it was possible to focus through the alumina and observe a copper-coloured film between the alumina and niobium. The greater extent of ceramic pullout in higher strength samples, and the tendency for higher strength samples to come from beams taken from block assembly edges may signal the combined beneficial effects of crowning of the blocks, and 'extrusion' of the liquid to the block edges due to the applied bonding pressure and capillary forces. Small solidified copper-coloured 'droplets' were found along the foil perimeter of the as-bonded block assembly, also indicative of some long-range redistribution of copper. However, even if it is assumed that all regions of pullout are caused by a thin intervening Cu layer, the area fraction of the interface with residual Cu is small, $\leq 30\%$, even in edge beams. In addition, Cu was not always apparent along the tensile edges of beams exhibiting high strength. (Samples were examined at magnifications of $\times 6$ to $\times 40$ using a stereographic microscope.) Thus the presence of residual copper does not appear to be a necessary condition for the formation of strong bonds.

Higher magnification SEM micrographs of the (interfacial) fracture regions show that a second phase decorates the interface, but to differing extents in high- and low-strength samples. Fig. 4 illustrates the metal (a, c) and ceramic (b, d) sides of the fracture surface of the 255 MPa (a, b) and 119 MPa (c, d) samples. The precipitates appear in two forms. 'Continuous' ribbons of precipitate outline a grain-like structure with an average apparent grain size of ≈ 60 μm. The scale of the grain structure does not match that of the ceramic. By repeatedly etching the metal side (and thereby also removing the second phase), it was deter-

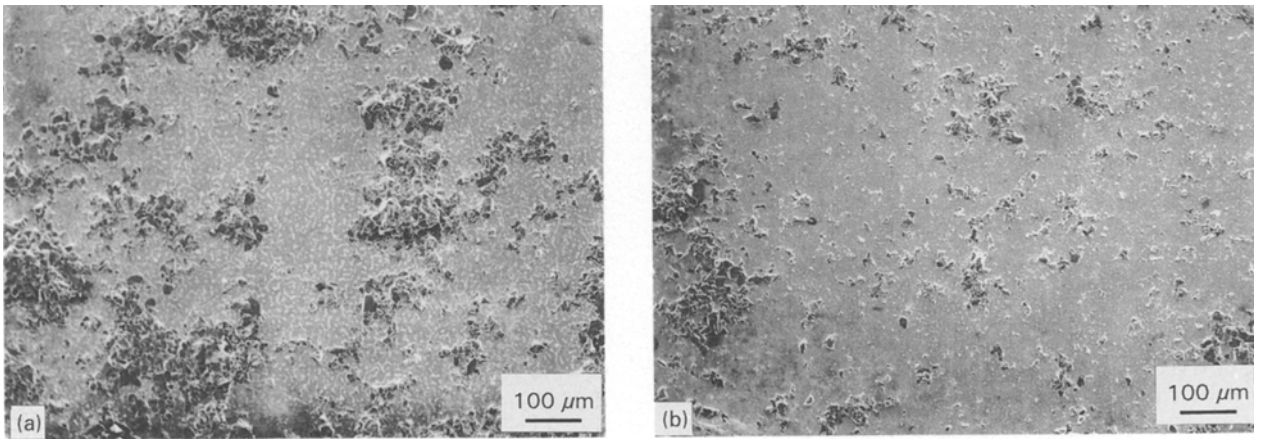

Figure 3 Metal side of fracture surface of as-bonded samples with (a) high strength (255 MPa) and (b) low strength (119 MPa), showing an increased degree of ceramic pullout in the higher-strength sample. The bottom edge is the tensile edge in both cases.

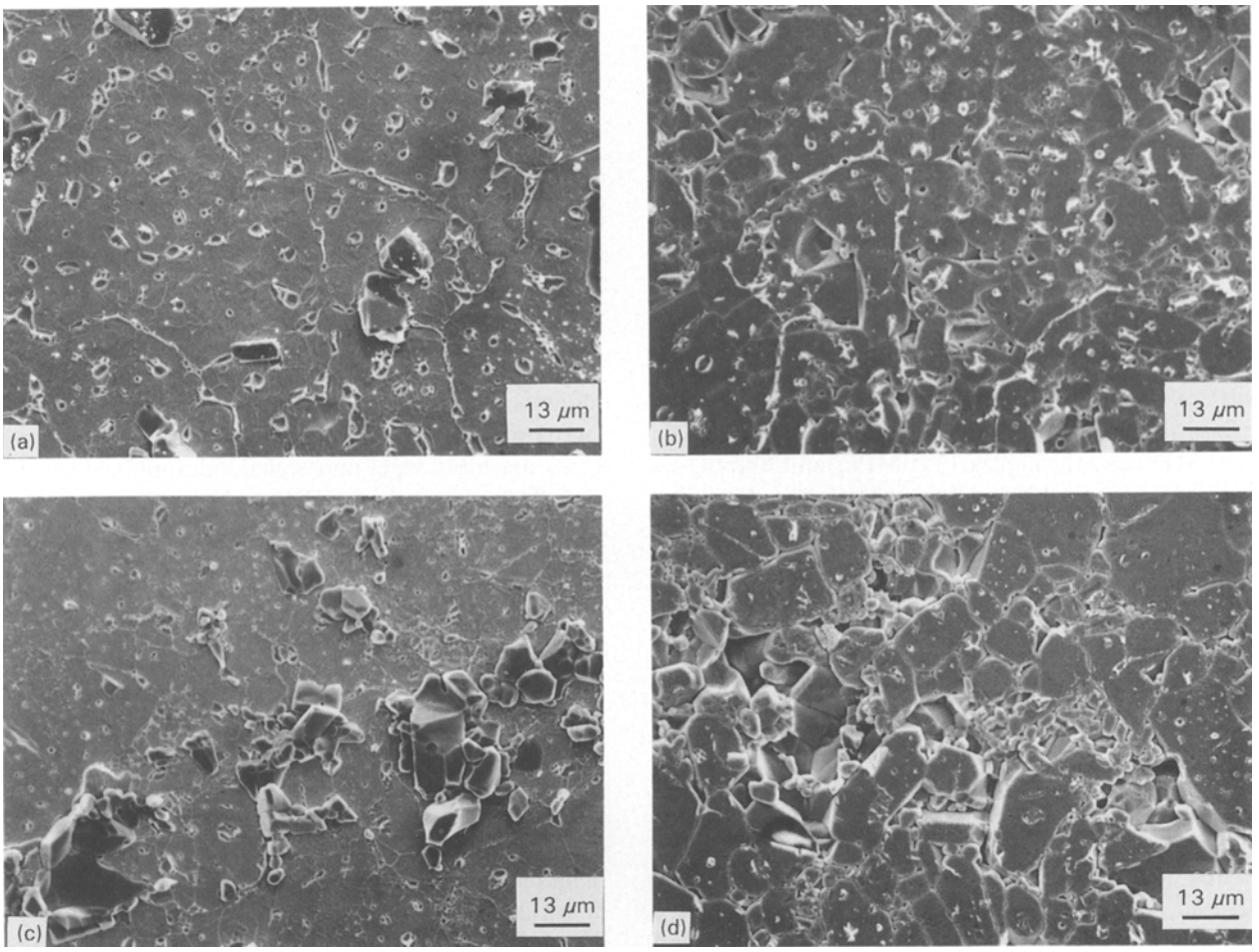

Figure 4 Exactly corresponding metal (a, c) and ceramic (b, d) fracture surfaces of as-bonded 255-MPa fracture stress (a, b) and 119-MPa (c, d) samples. Precipitates are present in two morphologies and evident in matching positions, indicating that failure occurs through the interfacial precipitate phase. The larger grains on the metal side are pulled-out alumina.

mined that the continuous network was located along the Nb grain boundaries. The precipitates are also present as a dispersed phase within the Nb grains along the interface. There is no obvious correlation between the position of these precipitates and any microstructural feature in the metal or ceramic. It is possible that the intragranular locations were dictated by an earlier finer-scale microstructure in the Nb foil; measurements indicate a grain size of ≈ 15 μm in the Nb foil prior to bonding, compared with a post-bonding grain size of ≈ 60 μm (Fig. 5a and b, respectively).

The presence of the precipitate phase at matching locations on both sides of the fracture surface suggests that the precipitate phase bonds well with both the alumina and the niobium, causing fracture to proceed through the phase. The precipitate phase is always more clearly defined and well developed in the samples that exhibit a higher fracture strength and a greater degree of ceramic failure, i.e. those nearer the block edges. The precipitates, however, cover a relatively small area fraction of the interface, and it is unlikely that they are the sole source of joint strength. Further reference to the micrographs of Fig. 4 reveals the replication of the alumina grain and pore structure onto the Nb foil, indicating that good ceramic/metal contact was achieved. Interfacial pores (unbonded regions) larger than those inherent to the alumina were not observed.

The chemistry of the interlayer, the fracture surfaces, and the second-phase particles were quantified using SEM and associated EDS analysis. Examination of specimens with intact bonds was limited to thin plates cut from the assembly edges where crowning and liquid redistribution effects would be exaggerated. Optical microscopy of such edge 'trim' plates revealed a thin copper-coloured film between the niobium and alumina along much of the Al_2O_3/interlayer interface. X-ray maps of the interlayer and Al_2O_3/interlayer interfacial region confirmed that the copper-coloured region was indeed copper-rich. SEM/EDS examination parallel to the alumina/interlayer interface of edge specimens revealed a non-uniform copper distribution. In regions where copper is detected, it is highly localized within a region only a few micrometres thick, comparable to or slightly greater than the average initial copper film thickness. In the edge plate examined, $\approx 75\%$ of the bond line showed the presence of a distinct copper layer. However, in the remaining 25% of the bond line, copper, if present, is in such a thin layer that it is not detectable by EDS. These results are consistent with the previously discussed observations on fracture surfaces indicating the presence of localized residual copper,

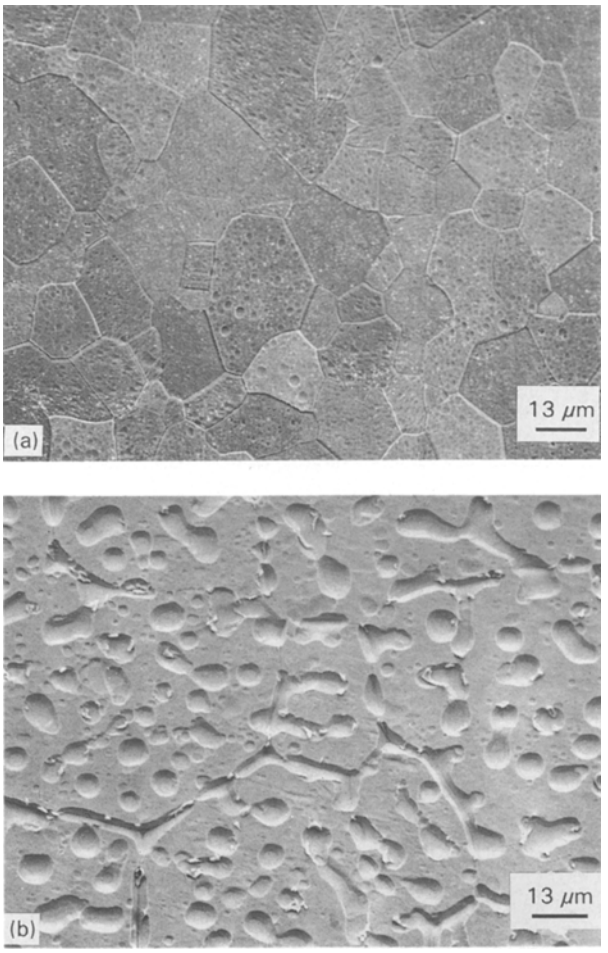

Figure 5 Microstructure of the Nb foil used (a) prior to bonding and (b) after bonding. In (b) the precipitate phase was removed by etching, causing the pits. It is evident that some of the precipitates formed along Nb grain boundaries.

and other indications of copper redistribution during bonding.

EDS line scans taken perpendicular to the interface indicate a transition layer from essentially pure Nb to alumina that is only a few micrometres thick, i.e. essentially the spatial resolution of the instrument. Liquid redistribution may have resulted in a local enhancement of the copper layer thickness at the edge; however even if some copper diffused into niobium, the results confirm that this diffusion occurs to only a limited extent at the processing temperatures used.

Precipitates in several different locations and of both morphologies were analysed on both the metal and ceramic sides of corresponding fracture surfaces. In both high-strength and low-strength samples, EDS results indicate that regardless of location and morphology, the precipitates contain Cu, Al, and O consistent with it being a copper aluminate. (Phase equilibria studies e.g. [58] in the Cu–Al–O system indicate that there are two copper aluminates, $CuAlO_2$ and $CuAl_2O_4$. Only the former co-exists in equilibrium with Al_2O_3 and Cu.) Both the Cu layer and the alumina substrate are reaction participants. The relative intensity of the Cu and Al peaks varies with location within the precipitate on the ceramic side. This is most probably a result of beam spreading and penetration, and thus varying contributions to the Al signal from the Al_2O_3. Analyses of the precipitate on the metal side show more consistent peak-height ratios, however the variation in chemistry was still large. For the majority of the precipitates, Si is also detected in small quantities (typically 1–4%), suggesting that the glassy phase in the alumina may also participate in interfacial reactions and the development of adhesion.

Analyses of Al_2O_3 surfaces in regions away from the precipitates (and patches of residual copper) show no Cu or Nb residue, only Al and O, and the matching sites on the Nb foil surface show no detectable Cu. This implies that in these regions, copper is removed from the interface by fluid flow owing to external and capillary pressures, and by reaction to form the precipitates. These results, coupled with the observed replication of the Al_2O_3 microstructure on the Nb foil, suggest that good direct bonding between the Nb foil and Al_2O_3 is achieved, and provide further evidence for both long-range and short-range redistribution of copper.

4.3. Contact angle measurements

To determine whether Nb has a beneficial impact on wetting, sessile drop experiments were conducted in vacuum at 1150 °C, and the contact angles formed by a pure Cu and a Nb-saturated Cu liquid droplet on alumina were measured. The phase diagram indicates that at the bonding temperature, a Nb-rich ($\approx$ 99 at % Nb) solid is in equilibrium with a Cu-rich ($\approx$ 98–99 at % Cu) liquid. The thermodynamic activity of Nb in the equilibrium liquid will thus be close to unity. Assuming that the added Nb dissolves and is uniformly distributed in the liquid at 1150 °C, this droplet approximates the liquid layer present during bonding. The Nb activity in the Nb-saturated Cu-rich solid solution at the post-bonding anneal temperature of 1000 °C will also be high. Therefore, if Nb acts as a reactive metal, one would expect a substantial effect.

The results are summarized in Fig. 6. Differences in the contact angles were evident almost immediately after melting. When 1150 °C was reached, the contact angle was $\approx 130°$ for pure copper, and $\approx 114°$ for Nb-saturated Cu. After 30 min at temperature, a slow decrease in the contact angle begins in the case of the Nb-saturated Cu. After 120 min the contact angle has decreased to 103°, and was still decreasing when observations were halted due to copper condensation on the viewing port. The cause of this progressive decrease in the contact angle is not known. In reactive metal braze systems such as Cu–Ag–Ti, a reaction product is formed, and enhances wetting [59]. In the present case, it is uncertain whether a constituent in the alumina (e.g. a glassy phase) is interacting with the Nb and being drawn to the surface, or whether some other time dependent change in the liquid–vapour or liquid–solid interfacial energy is responsible. Recent work with polycrystals of varying purity and sapphire (K. Nakashima, A. P. Tomsia and A. M. Glaeser, unpublished data) has shown similar decreases in contact angle regardless of the purity of the alumina used. We speculate that in the sessile drop experiments

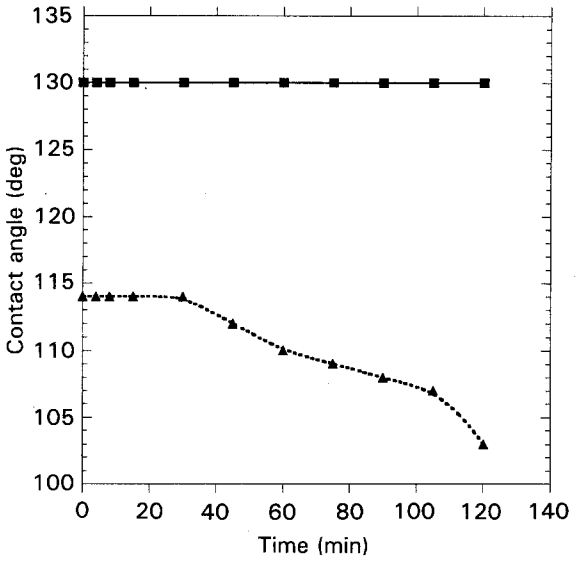

Figure 6 Time dependence of the contact angle (defined from within the drop) of ■, pure Cu and ▲ Cu–2 wt % Nb on an alumina substrate at a temperature of 1150 °C. With Nb the contact angle is lower than for pure copper, and decreases with time.

preferential evaporation of copper supersaturates the liquid with respect to Nb and may be inducing deposition of Nb at the Al_2O_3/interlayer interface. During joining, consumption of Cu by the formation of the precipitates may have a similar effect.

4.4. Effect of post-bonding annealing

One of the objectives of designing PTLP bonding interlayers is to facilitate the production of joints that can sustain use at elevated temperature. In the present study, an unabsorbed copper-rich phase is retained within isolated regions along some portions of the Al_2O_3/interlayer interface, and the high-temperature capabilities of a more completely homogenized (or fully reacted) interlayer were potentially compromised. However, to allow a comparison with the behaviour of Cu/Pt/Cu interlayer bonded Al_2O_3, the effect of a 10-h anneal at 1000 °C (0.937 T_m of Cu) in high-purity, low oxygen content argon on subsequent room temperature strength was assessed.

In Cu/Pt/Cu interlayer bonded Al_2O_3, microstructural evaluation of fracture surfaces suggested that exposure to a low oxygen partial pressure atmosphere caused solid-state interfacial dewetting of metal at the interlayer/ceramic interface. Annealing of these assemblies in gettered argon caused a severe loss of strength [1] (Fig. 2). In view of the potential for limited diffusion of Cu into Nb and incomplete reaction, the reportedly rapid diffusion of oxygen in copper at 1000 °C [36] and in Nb, and the indication of a pronounced effect of oxygen content on the strength of copper/alumina interfaces [39], a similar loss of strength was possible in the current study. However, for the Cu/Nb/Cu bonded alumina, only a slight loss of strength compared to the as-bonded material (with similar polishing history) was evident (Table I and Fig. 2). In addition, comparisons of the fracture surfaces showed a substantial degree of ceramic pullout in annealed samples (Fig. 7a) at a higher level than in the

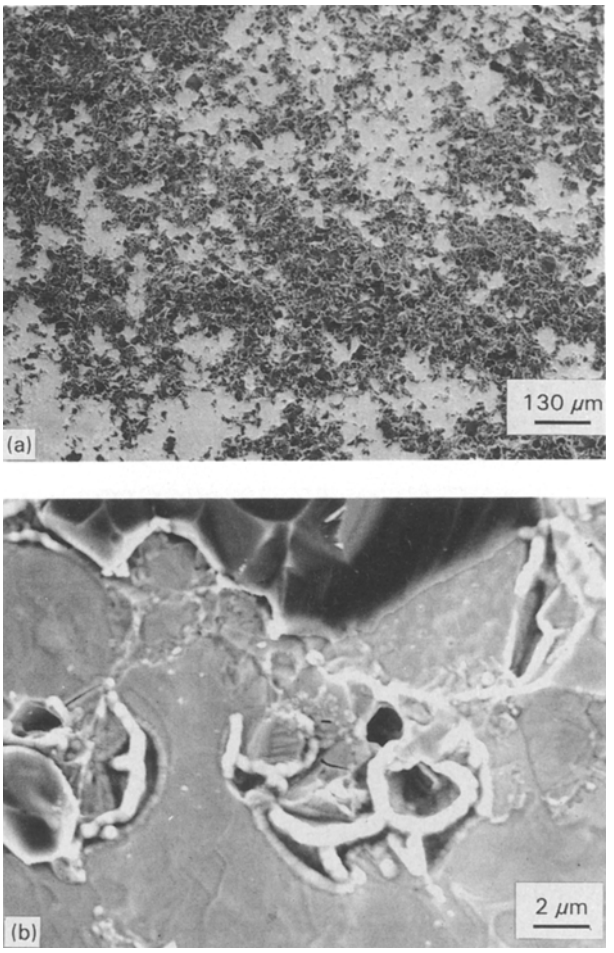

Figure 7 Metal side of fracture surface of a sample given a post-bonding anneal treatment at (a) low and (b) higher magnification. A substantial degree of ceramic pullout is evident in (a). Si detected at the edges of regions such as those shown in (b) suggest that the glassy phase within the alumina may play a role in modifying the adhesion between the ceramic and metal.

high strength, as-bonded samples (Fig. 3a). EDS analysis of the metal fracture surfaces of Ar-annealed samples revealed regions of significantly increased Si concentration located mainly around the perimeter of pull-out zones. The results suggest that the alumina glassy phase is drawn to the interface during the post-bonding anneal and may play a role in determining subsequent fracture behaviour (Fig. 7b).

Several factors are believed to contribute to the difference in the response of Cu/Pt/Cu and Cu/Nb/Cu interlayer bonded assemblies to exposure to low oxygen partial pressure environments. In the case of Cu/Pt/Cu, no precipitate phase is formed during bonding, and the metal foil in contact with the alumina is a Pt-rich Cu–Pt solid solution. In the case of Cu/Nb/Cu interlayer bonded alumina, copper is found in the interfacial region in the form of isolated patches of a copper-rich alloy, and in the form of copper-containing precipitates.

In the regions near the block perimeter, where undissolved and unreacted copper is present, behaviour paralleling that in Cu/Pt/Cu specimens might occur. However, Nb has been cited along with Ti, V, Cr, Zr, Mo, Hf, Ta, and W as an 'active' metal. The wetting experiments indicate that Nb dissolved in Cu

promotes wetting of the alumina during initial bond formation at 1150 °C. Poor interfacial contact was evident in the lower strength Cu/Pt/Cu assemblies. The finding that Nb improves the wetting behaviour of copper may explain the absence of large unbonded regions on fracture surfaces, and thereby contribute to the higher average strength and narrower strength distribution relative to the Cu/Pt/Cu interlayer bonded assemblies. We speculate that dissolved Nb also counters the effects of a loss of oxygen on the wetting behaviour during post-bonding annealing.

5. Discussion

The results show that strengths in the PTLP bonded assemblies approach those of similar size $Al_2O_3/Nb/Al_2O_3$ samples prepared by diffusion bonding at 1450 °C (B. J. Dalgleish, unpublished data), and nearly reach those of the ceramic. The potential for achieving high joint strength at a substantially lower processing temperature is indicated. In contrast to results obtained using Cu/Pt/Cu interlayers, little residual interfacial porosity was found.

Fig. 8 illustrates a possible developmental sequence of interfacial microstructures that appears consistent with the observations. The roughness of the Nb foil and alumina substrates, exaggerated in scale in Fig. 8, coupled with the application of pressure should cause short-range redistribution of the liquid, and locally bring Nb and Al_2O_3 into closer proximity or even direct contact. If the liquid wets the Nb/Al_2O_3 interface, a thin intervening Cu-rich liquid layer will persist. The capillary forces and applied pressure will drive flow of Nb out from the contact points and cause deposition of Nb in the liquid-filled cavities along the interface. This should also tend to make the foil conform to the shape of the alumina, possibly transferring the surface microstructure of the alumina to the Nb foil. However, transport along the Nb/Al_2O_3 interface may be enhanced even in the absence of a fully wetting layer; an equilibrium segregation layer of Cu at the Nb/Al_2O_3 interface may enhance the interfacial transport rate relative to that for pure Nb/Al_2O_3 interfaces, and increase the role of solid-state diffusion in bond formation (e.g. as occurs in Ni-activated sintering of W [60]). Both of these transport mechanisms will induce centre-to-centre approach, and may induce extrusion of the liquid to the perimeter of the bond plane. The EDS results suggest (but do not prove) that direct contact and bonding between Nb and Al_2O_3 is achieved; Auger analysis of fracture surfaces or TEM of cross sections would be required to preclude the presence of a thin Cu layer between Nb and Al_2O_3.

If essentially direct contact between the Nb and Al_2O_3 is achieved, an additional driving force may arise for the transport of Nb along the surface of the liquid 'pockets', from regions of negative curvature to regions of more intensely negative curvature. This driving force will be higher the smaller the contact angle that Nb forms on Al_2O_3 in the presence of the Cu-rich liquid. The liquid pocket will attempt to develop an equilibrium shape dictated by the relative

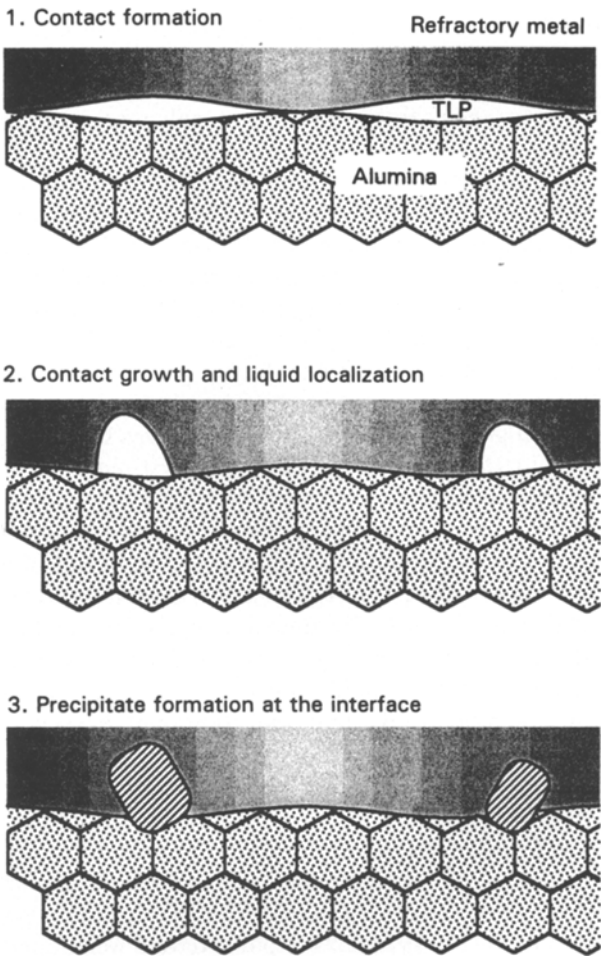

Figure 8 Schematic illustration of possible developmental sequence of interfacial microstructures. Roughness causes short-range redistribution of liquid and direct contact between foil and ceramic. Transport of Nb through the liquid phase, or possibly along the Al_2O_3/Nb interface, causes growth of the contact area. Reaction between Cu, Al_2O_3 and additional oxygen causes the formation of precipitates.

interfacial energies at the Nb–Al_2O_3–Cu(Nb) triple junction. This evolution of shape can contribute to an increase in contact area, and bond strength, but produces no centre-to-centre approach. With the liquid layer, no centre-to-centre approach is necessary to eliminate the porosity unless the surface is too rough. However, if the alumina blocks are crowned, enough centre-to-centre approach is required to establish some contact points in the edge region, either by plastic deformation during assembly or by solution-reprecipitation.

The capillary forces associated with the liquid–vapour meniscus will try to pull the Nb and Al_2O_3 into direct contact, driving both short- and long-range redistribution of liquid, if, as seems likely, $(\theta_1 + \theta_2) \leq \pi$, where θ_1 and θ_2 are the contact angles for the liquid on the ceramic and Nb, respectively. This is the condition under which the liquid between two flat plates spreads and thins indefinitely, rather than reaching an equilibrium thickness of zero capillary force. Thus, if this condition is met, capillary forces alone would assuredly drive the long-range liquid redistribution in response to the substrate crowning. The data in Fig. 6 show that $\theta_1 \leq 114°$ for the Cu(Nb)

liquid, requiring only that $\theta_2 \leq 56°$ to satisfy this condition. This latter value would certainly obtain in a pure Nb/Cu system [61], but in the presence of the higher oxygen content here, it may only marginally be met.

Whichever combination of these mechanisms is operative, they result in the growth of the contact area and ultimate localization of the Cu-rich liquid. In the present case, there is the aforementioned additional complication: localization of the liquid is accompanied by or followed by the formation of precipitates containing Cu, Al, and O. The Nb grain boundaries may serve as preferred nucleation sites for two reasons: (i) grain boundary grooving localizes the liquid, and (ii) the presence of the boundary reduces the nucleation barrier.

The formation of precipitates is somewhat unexpected. Their formation is apparently the result of a reaction involving Cu, Al_2O_3, and additional oxygen. Neither Cu nor Nb will reduce alumina to any significant extent at the bonding temperature, and thus little dissolved oxygen would be generated in this way. It appears more likely that the additional oxygen is incorporated into the Cu coating during deposition, or that the Nb foil contains sufficient dissolved oxygen for it to be reactive at the low bonding temperature used. (Similar considerations arose in rationalizing the formation of nickel aluminate spinel phase during PTLP bonding of Al_2O_3 with Cu/Ni/Cu multilayer interlayers [2]. As regions of poor wetting were found in this system, and the beneficial effects of dissolved oxygen on wetting are well known, this suggests that the amount of oxygen incorporated in the film must be well below the quantity required to form the $Cu–Cu_2O$ eutectic liquid.) As a result of the incorporation of additional oxygen, in the outer regions, where more Cu is available as a result of fluid flow prior to extensive reaction, residual copper is found, and more precipitates form. In the interior, where little copper remained, sufficient oxygen was supplied to completely consume the copper.

The data unequivocally show that the bars from three of the edges of the block are stronger probably as a result of several factors. There is some indication that some damage was done during the more extensive polishing and cleaning of the interior plates. However, there is further reason to believe that the edge plates were inherently stronger as well owing to composition differences. This is suggested by the greater amount of ceramic pull-out evident over most of the fracture surface for the bars from around the edges than those from the middle. Such an observation could be consistent with the presence of more copper in the bonds from edge-bars owing to the copper redistribution caused by crowning (and supposing that the blocks tilted just enough that the region of close approach occurred nearer one edge). The fact that even the edge beams from the more heavily polished interior plates are weaker than all the beams from the less extensively polished edge plates seems to affirm that the additional polishing did have some adverse effect.

The extra copper could, in principle, lead to increased fracture resistance owing to the reaction phase which forms, and may be strong enough to bridge the crack. Alternatively, the several micrometres of free copper could impart some increased local ductility which effectively increases the toughness (assuming the Cu has a lower yield stress than the Nb in the presence of the O impurity). Finally, there may be better bonding at the Nb/Al_2O_3 interfaces owing to atomic levels of Cu and O impurities segregated there. Prior studies of failure in pure Nb/Al_2O_3 assemblies indicate that fracture is purely interfacial [9–12; B. J. Dalgleish, unpublished data]. (In recent work of D. Korn and G. Elssner (unpublished data), mixed interface and ceramic fracture has been observed in single crystal Nb/sapphire bonds for the orientations giving the highest fracture energies.) Prior studies of failure in pure Cu/Al_2O_3 assemblies indicate a tendency for ceramic failure and ceramic pullout in well-bonded assemblies [e.g. 35, 59]. These observations would be consistent with the suggestion that the Cu/alumina bond is tougher than the Nb/alumina bond, owing either to better atomic bonding or to greater plasticity owing to a lower yield stress in the Cu/Al_2O_3 bonds. These several possible reasons are presently unresolvable, but merit further study in order to reveal methods to attain stronger bonds within this system.

Although the underlying mechanism for the decrease in contact angle is not known at present, the fact remains that Nb does decrease the contact angle relative to that for pure copper, and improves wetting. Even if only the short-time contact angle of 114° (rather than the lower values that arise with increasing time) is pertinent to bonding, elimination of interfacial porosity should occur more rapidly than with higher contact angle pure Cu. We anticipate that the decrease in contact angle will also manifest itself in a greater resistance to solid-state dewetting. Collectively, these factors would improve the strength distribution in as-processed samples, and would be expected to reduce the effects of exposure to a reducing environment at elevated temperature. (It is recognized that although Nb may enhance the interfacial bonding of Cu to Al_2O_3, it is to be expected, (e.g. from work with Ag/Nb [63]) that Cu may reduce the strength relative to that for pure Nb/Al_2O_3, an effect needing further study.)

An additional, potentially important difference between the Cu/Pt and Cu/Nb experiments is the concentration and thermodynamic activity of Cu at the interface during bonding. The relatively high concentration and activity of Cu in the Cu/Nb case make reaction between Cu and Al_2O_3 more likely than in the Cu/Pt case, and the low rate of incorporation of Cu into Nb maintains Cu at a high activity. Thus if conditions for reaction between Cu and Al_2O_3 are favourable, one can anticipate that reaction will proceed until all the Cu has been depleted, and the small amount of Nb present in the liquid has precipitated onto either the Nb foil or the ceramic. This scenario may rationalize the absence of any detectable copper on either the metal or ceramic side of corresponding fracture surfaces where the precipitate phase is well developed.

The tendency for a greater degree of ceramic failure and a slight loss of strength after argon annealing is interesting. It suggests a degradation of the alumina as a result of the annealing. In principle, an interaction between constituents of the glassy phase and either Cu or Nb that results in microstructural degradation of the intergranular glassy film, and thereby intergranular adhesion in the alumina, could account for the change in fracture characteristics. This would be consistent with the observation of an enhanced Si concentration around the perimeter of pull-out zones. It is possible that such changes would have been evident in Cu/Pt had other factors such as interfacial dewetting not had an even more potent influence. Further investigation of this behaviour is planned.

6. Conclusions

The results indicate that, as in the case of Pt/Al_2O_3 bonding, high-strength joints between Nb and Al_2O_3 can be produced at significantly lower temperatures than those previously used for diffusion bonding by introducing a thin intervening layer of Cu. Compared to Cu/Pt/Cu interlayer bonded Al_2O_3, fracture strengths were generally higher and less scattered. Sessile drop experiments comparing the wetting behaviour of Cu and Nb-saturated Cu on alumina indicate that Nb acts to decrease the Cu contact angle, and this is thought to promote a more favourable strength distribution than obtained with Cu/Pt-based interlayers. More generally, the results suggest that precoating substrates with a thin layer of a reactive metal may improve the degree of contact between the transient liquid and the substrate, and thereby increase the average strength, narrow the strength distribution, or both.

Fractographic studies and microchemical analysis suggest that several factors affect the strength and fracture characteristics of as-bonded assemblies. Evidence suggests that long-range redistribution of copper occurred during bonding, most likely as a result of polishing-induced crowning of the Al_2O_3 blocks, and the high bonding pressure used. In (edge) beams where residual unreacted and unabsorbed Cu is more common, the degree of ceramic pullout is increased. However, the degree of pullout in stronger as-bonded samples and the extent of interfacial coverage by Cu appears to be too low for either to account for the high strength. As Cu was not always found along the tensile edges of strong beams, the presence of residual copper does not appear to be a necessary condition for the formation of strong bonds. There is a stronger positive correlation between the fracture strength and the degree of precipitate development at the interface. Higher strengths, and a greater tendency towards ceramic pullout were observed in samples where the precipitate was more extensive. Spatial variability in the extent of precipitate development correlates with spatial variations in the local copper film thickness caused by redistribution. The second phase appears to bond strongly to both the Al_2O_3 and Nb, and bridges the ceramic/metal interface; fracture progresses through the second phase. However, the results of semiquantitative analyses, and the observed replication of the alumina grain structure on the Nb foil suggest that direct bonding between Nb and Al_2O_3 provides a significant fraction of the measured joint strength.

There is also an indication that excessive polishing (and/or associated cleaning techniques) of the bonded samples degrades strength. However, further study of this phenomenon will be required in samples where copper redistribution effects are less important. EDS analysis shows that the precipitate phase contains copper, aluminium, and oxygen. Precipitate formation involves a reaction between Cu, Al_2O_3, and additional oxygen. The precipitate appears in two distinct forms, continuous and discrete, with the continuous form appearing to form preferentially along Nb grain boundaries. This suggests that a refinement of the Nb grain size could promote the formation of a more uniform distribution of the bridging interfacial reaction product. Furthermore, the results indicate the potential for designing joining processes in which the transient liquid former is removed by a reaction that yields a more refractory product.

In contrast to behaviour observed in Cu/Pt/Cu bonded assemblies, post-bonding anneals at 1000 °C in gettered argon caused only a minor decrease in flexure strength, and an increased tendency for ceramic pullout and failure. This difference in response is most likely due to the differences in the chemical form and distribution of Cu in the two cases. In as-bonded Cu/Pt/Cu, the Cu is present in solid solution and at its highest concentration uniformly along the interface. Decreases in the oxygen content have the potential to affect the entire bonded interface. In as-bonded Cu/Nb/Cu assemblies, Cu is present primarily in the form of precipitates in interior beams, and in edge beams these are supplemented by patches of unreacted copper. Reduction of the precipitates would introduce only small interfacial flaws. In those regions where unreacted copper is present, Nb (present at low concentrations but high chemical activity) may play a role in countering the deleterious effects of oxygen depletion on the wetting and adhesion characteristics of a copper-rich film on Al_2O_3.

Acknowledgements

This research program was initiated while A. M. Glaeser was on appointment as a Miller Research Professor in the Miller Institute for Basic Research in Science. Helpful discussions and correspondences with Y. Iino, M. Koizumi, M. G. Nicholas, J. A. Pask, and R. O. Ritchie are acknowledged. Special thanks are due to the Alcoa Foundation for providing the financial resources that allowed the initial demonstration of this concept. Additional unrestricted grants from and equipment donations by ARCO, IBM, and DuPont contributed to the development of facilities used in this research. This research was supported by the Director, the Office of Energy Research, Office of Basic Energy Sciences, Materials Sciences Division of the U.S. Department of Energy under Contract No. DE-AC03-76SF00098.

References

1. M. L. SHALZ, B. J. DALGLEISH, A. P. TOMSIA and A. M. GLAESER, *J. Mater. Sci.* **28** (1993) 1673.
2. *Idem, ibid* (in press).
3. W. G. NICHOLAS and D. A. MORTIMER, *Mater. Sci. Tech.* **1** (1985) 657.
4. A. J. MOORHEAD, *Adv. Ceram. Mater.* **2** (1987) 159.
5. K. SUGANUMA, Y. MIYAMOTO and M. KOIZUMI, *Ann. Rev. Mater. Sci.* **18** (1988) 47.
6. R. V. ALLEN and W. E. BORBIDGE, *J. Mater. Sci.* **18** (1983) 2835.
7. F. P. BAILEY and W. E. BORBIDGE, in "Surfaces and Interfaces in Ceramic and Ceramic–metal Systems", (Materials Research, 14), edited by J. A. Pask and A. G. Evans (Plenum, New York, 1981) p. 525.
8. G. ELSSNER and G. PETZOW, *Z. Metallkde.* **64** (1973) 280.
9. G. ELSSNER, S. RIEDEL, and R. PABST, *Praktische Metallographie* **12** (1975) 234.
10. M. TURWITT, G. ELSSNER and G. PETZOW, *J. de Physique* **46** (1985) C4-123.
11. A. G. EVANS, M. RÜHLE and M. TURWITT, *ibid.* **46** (1985) C4-613.
12. H. F. FISCHMEISTER, W. MADER, B. GIBBESCH and G. ELSSNER, in "Interfacial Structures, Properties and Design", edited by M. H. Yoo, W. A. T. Clark and C. L. Braint (*Mater. Res. Soc. Proc.*, **122,** Pittsburgh, Pennsylvania 1988) p. 529.
13. B. DERBY, in "Ceramic Microstructures 86", edited by J. A. Pask and A. G. Evans (Plenum, New York, 1987) p. 319.
14. B. DERBY, in "Joining of Ceramics", edited by M. Nicholas, (Chapman & Hall, London, 1990) p. 94.
15. J. KLOMP, in "Science of Ceramics", Vol. 5, edited by C. Brosset and E. Knopp (Swedish Institute for Silicate Research, Gothenburg, 1970) p. 501.
16. YU. V. NAIDICH and V. S. ZHURAVLEV, *Refractories (USSR)* **15** (1974) 55.
17. M. KOIZUMI, M. TAKAGI, K. SUGANUMA, Y. MIYAMOTO and T. OKAMOTO, in "High Tech Ceramics", edited by P. Vincenzini (Elsevier Science Publishers, Amsterdam, 1987) p. 1033.
18. Y. IINO and N. TAGUCHI, *J. Mater. Sci. Lett.* **7** (1988) 981.
19. D. S. DUVALL, W. A. OWCZARSKI and D. F. PAULONIS, *Welding J.* **53** (1974) 203.
20. R. E. LOEHMAN, in "Surfaces and Interfaces in Ceramic and Ceramic-metal Systems", edited by J. A. Pask and A. G. Evans (Plenum, New York, 1981) p. 701.
21. R. D. BRITTAIN, S. M. JOHNSON, R. H. LAMOREAUX and D. J. ROWCLIFFE, *J. Amer. Ceram. Soc.* **67** (1984) 522.
22. M. L. MECARTNEY, R. SINCLAIR and R. E. LOEHMAN, *J. Amer. Ceram. Soc.* **68** (1985) 472.
23. S. M. JOHNSON and D. J. ROWCLIFFE, *ibid.* **68** (1985) 468.
24. S. BAIK and R. RAJ, *ibid.* **70** (1987) C105.
25. T. ISEKI, K. YAMASHITA and H. SUZUKI, *ibid.* **64** (1981) C-13.
26. T. ISEKI, K. YAMASHITA and H. SUZUKI, *Proc. Brit. Ceram. Soc.* **31** (1981) 1.
27. L. BERNSTEIN and H. BARTHOLOMEW, *Trans. AIME* **236** (1966) 405.
28. Y. IINO, *J. Mater. Sci. Lett.* **10** (1991) 104.
29. M. L. SHALZ, B. J. DALGLEISH, A. P. TOMSIA and A. M. GLAESER, *Ceramic Transactions*, **35** (1993) 301.
30. A. M. GLAESER, M. L. SHALZ, B. J. DALGLEISH and A. P. TOMSIA, *Ceramic Trans.* **34** (1993) 341.
31. C. A. M. MULDER and J. T. KLOMP, *J. de Physique* **46** (1985) C4-111.
32. VON W. DAWIHL and E. KLINGLER, *Ber. Deutsch. Keram. Gesell.* **46** (1969) 12.
33. G. HEIDT and G. HEIMKE, *ibid.* **50** (1973) 303.
34. G. HEIDT and G. HEIMKE, *J. Mater. Sci.* **10** (1975) 887.
35. R. M. CRISPIN and M. G. NICHOLAS, *Ceram. Eng. Sci. Proc.* **10** (1989) 1575.
36. C. BERAUD, M. COURBIERE, C. ESNOUF, D. JUVE and D. TREHEUX, *J. Mater. Sci.* **24** (1989) 4545.
37. M. NICHOLAS, R. R. D. FORGAN and D. M. POOLE, *J. Mater. Sci.* **3** (1968) 9.
38. M. WITTMER, C. R. BOER, P. GUDMUNDSON and J. CARLSSON, *J. Amer. Ceram. Soc.* **65** (1982) 149.
39. Y. YOSHINO, *ibid.* **72** (1989) 1322.
40. S. T. KIM and C. H. KIM, *J. Mater. Sci.* **27** (1992) 2061.
41. S. MOROZUMI, M. KIKUCHI and T. NISHINO, *ibid.* **16** (1981) 2137.
42. M. FLORJANCIC, W. MADER, M. RÜHLE, and M. TURWITT, *J. de Physique* **46** (1985) C4-129.
43. M. RÜHLE, K. BURGER and W. MADER, *J. Microsc. Spectrosc. Electron.* **11** (1986) 163.
44. K. BURGER, W. MADER, and M. RÜHLE, *Ultramicroscopy* **22** (1987) 1.
45. M. RÜHLE, M. BACKHAUS-RICOULT, K. BURGER and W. MADER, in "Ceramic Microstructures 86", edited by J. A. Pask and A. G. Evans (Plenum, New York, 1987) p. 295.
46. Y. ISHIDA, H. ICHINOSE, J. WANG and T. SUGA, in Proceedings of the 46th Annual Meeting of EMSA, edited by G. W. Bailey (San Francisco Press, San Francisco, 1988) p. 728.
47. B. GIBBESCH, G. ELSSNER, W. MADER and H. FISCHMEISTER, *Ceram. Eng. Sci. Proc.* **10** (1989) 1503.
48. F. S. OHUCHI, *J. Mater. Sci. Lett.* **8** (1989) 1427.
49. K. BURGER and M. RÜHLE, *Ceram. Eng. Sci. Proc.*. **10** (1989) 1549.
50. M. KUWABARA, J. C. H. SPENCE and M. RÜHLE, *J. Mater. Res.* **4** (1989) 972.
51. K. BURGER and M. RÜHLE, *Ultramicroscopy* **29** (1989) 88.
52. W. MADER and M. RÜHLE, *Acta Metall.* **37** (1989) 853.
53. J. MAYER, C. P. FLYNN and M. RÜHLE, *Ultramicroscopy* **33** (1990) 51.
54. T. B. MASSALSKI, ed., "Binary Alloy Phase Diagrams", Vol. 2 (ASM International, Metals Park, Ohio, 1990) p. 1440.
55. R. P. ELLIOT, "Constitution of Binary Alloys, First Supplement", (McGraw-Hill, New York, 1965) p. 253.
56. B. J. DALGLEISH, M. C. LU and A. G. EVANS, *Acta Metall.* **36** (1988) 2029.
57. H. C. CAO, M. D. THOULESS and A. G. EVANS, *ibid.* **36** (1988) 2037.
58. A. M. M. GADALLA and J. WHITE, *Trans. Brit. Ceram. Soc.* **63** (1964) 39.
59. R. E. LOEHMAN and A. P. TOMSIA, *Amer. Ceram. Soc. Bull.* **67** (1988) 375.
60. A. L. PRILL, H. W. HAYDEN and J. H. BROPHY, *Trans. AIME* **230** (1964) 769.
61. O. F. DE LIMA, M. KREHL and K. SCHULZE, *J. Mater. Sci.* **20** (1985) 2464.
62. R. O. RITCHIE, R. M. CANNON JR., B. J. DALGLEISH, R. H. DAUSKARDT, and J. McNANEY, *Mater. Sci. Engng*, (in press).
63. D. KORN, G. ELSSNER, H. F. FISCHMEISTER and M. RÜHLE, *Acta Metall. Mater.* **40** (1992) 5355.

Received 6 September
and accepted 25 November 1993